EUROPEAN ORGANIZATION FOR NUCLEAR RESEARCH

CERN-EP/2000-106
July 26, 2000

Measurement of the $\bar{B}^0$ and B^- Meson Lifetimes

The ALEPH Collaboration

Abstract

The lifetimes of the $\bar{B}^0$ and B^- mesons are measured using a sample of about four million hadronic Z decays collected from 1991 to 1995 with the ALEPH detector at LEP. The data sample has been recently reprocessed, achieving a substantial improvement in the tracking performance. Semileptonic decays of $\bar{B}^0$ and B^- mesons are partially reconstructed by identifying events containing a lepton with an associated $D^{\star+}$ or D^0 meson. The proper time of the B meson is estimated from the measured decay length and the momentum of the D-lepton system. A fit to the proper time of 1880 $D^{\star+}\ell^-$ and 2856 $D^0\ell^-$ candidates yields the following results:

$$\begin{aligned} \tau_{\bar{B}^0} &= 1.518 \pm 0.053 \pm 0.034 \text{ ps}, \\ \tau_{B^-} &= 1.648 \pm 0.049 \pm 0.035 \text{ ps}, \\ \tau_{B^-}/\tau_{\bar{B}^0} &= 1.085 \pm 0.059 \pm 0.018. \end{aligned}$$

(Submitted to Physics Letters)

The ALEPH Collaboration

R. Barate, D. Decamp, P. Ghez, C. Goy, J.-P. Lees, E. Merle, M.-N. Minard, B. Pietrzyk

Laboratoire de Physique des Particules (LAPP), IN^{2}P^3-CNRS, F-74019 Annecy-le-Vieux Cedex, France

S. Bravo, M.P. Casado, M. Chmeissani, J.M. Crespo, E. Fernandez, M. Fernandez-Bosman, Ll. Garrido,[15] E. Graugés, M. Martinez, G. Merino, R. Miquel, Ll.M. Mir, A. Pacheco, H. Ruiz

Institut de Física d'Altes Energies, Universitat Autònoma de Barcelona, E-08193 Bellaterra (Barcelona), Spain[7]

A. Colaleo, D. Creanza, M. de Palma, G. Iaselli, G. Maggi, M. Maggi,[1] S. Nuzzo, A. Ranieri, G. Raso,[23] F. Ruggieri, G. Selvaggi, L. Silvestris, P. Tempesta, A. Tricomi,[3] G. Zito

Dipartimento di Fisica, INFN Sezione di Bari, I-70126 Bari, Italy

X. Huang, J. Lin, Q. Ouyang, T. Wang, Y. Xie, R. Xu, S. Xue, J. Zhang, L. Zhang, W. Zhao

Institute of High Energy Physics, Academia Sinica, Beijing, The People's Republic of China[8]

D. Abbaneo, G. Boix,[6] O. Buchmüller, M. Cattaneo, F. Cerutti, G. Dissertori, H. Drevermann, R.W. Forty, M. Frank, T.C. Greening, J.B. Hansen, J. Harvey, P. Janot, B. Jost, I. Lehraus, P. Mato, A. Minten, A. Moutoussi, F. Ranjard, L. Rolandi, D. Schlatter, M. Schmitt,[20] O. Schneider,[2] P. Spagnolo, W. Tejessy, F. Teubert, E. Tournefier, A.E. Wright

European Laboratory for Particle Physics (CERN), CH-1211 Geneva 23, Switzerland

Z. Ajaltouni, F. Badaud, G. Chazelle, O. Deschamps, A. Falvard, P. Gay, C. Guicheney, P. Henrard, J. Jousset, B. Michel, S. Monteil, J-C. Montret, D. Pallin, P. Perret, F. Podlyski

Laboratoire de Physique Corpusculaire, Université Blaise Pascal, IN^{2}P^3-CNRS, Clermont-Ferrand, F-63177 Aubière, France

J.D. Hansen, J.R. Hansen, P.H. Hansen,[1] B.S. Nilsson, A. Wäänänen

Niels Bohr Institute, DK-2100 Copenhagen, Denmark[9]

G. Daskalakis, A. Kyriakis, C. Markou, E. Simopoulou, A. Vayaki

Nuclear Research Center Demokritos (NRCD), GR-15310 Attiki, Greece

A. Blondel,[12] G. Bonneaud, J.-C. Brient, A. Rougé, M. Rumpf, M. Swynghedauw, M. Verderi, H. Videau

Laboratoire de Physique Nucléaire et des Hautes Energies, Ecole Polytechnique, IN^{2}P^3-CNRS, F-91128 Palaiseau Cedex, France

E. Focardi, G. Parrini, K. Zachariadou

Dipartimento di Fisica, Università di Firenze, INFN Sezione di Firenze, I-50125 Firenze, Italy

A. Antonelli, M. Antonelli, G. Bencivenni, G. Bologna,[4] F. Bossi, P. Campana, G. Capon, V. Chiarella, P. Laurelli, G. Mannocchi,[5] F. Murtas, G.P. Murtas, L. Passalacqua, M. Pepe-Altarelli

Laboratori Nazionali dell'INFN (LNF-INFN), I-00044 Frascati, Italy

A.W. Halley, J.G. Lynch, P. Negus, V. O'Shea, C. Raine, P. Teixeira-Dias, A.S. Thompson

Department of Physics and Astronomy, University of Glasgow, Glasgow G12 8QQ,United Kingdom[10]

R. Cavanaugh, S. Dhamotharan, C. Geweniger,[1] P. Hanke, G. Hansper, V. Hepp, E.E. Kluge, A. Putzer, J. Sommer, K. Tittel, S. Werner,[19] M. Wunsch[19]

Kirchhoff-Institut fi̇r Physik, Universität Heidelberg, D-69120 Heidelberg, Germany[16]

R. Beuselinck, D.M. Binnie, W. Cameron, P.J. Dornan, M. Girone, N. Marinelli, J.K. Sedgbeer, J.C. Thompson,[14] E. Thomson[22]

Department of Physics, Imperial College, London SW7 2BZ, United Kingdom[10]

V.M. Ghete, P. Girtler, E. Kneringer, D. Kuhn, G. Rudolph

Institut für Experimentalphysik, Universität Innsbruck, A-6020 Innsbruck, Austria[18]

C.K. Bowdery, P.G. Buck, A.J. Finch, F. Foster, G. Hughes, R.W.L. Jones, N.A. Robertson

Department of Physics, University of Lancaster, Lancaster LA1 4YB, United Kingdom[10]

I. Giehl, K. Jakobs, K. Kleinknecht, G. Quast,[1] B. Renk, E. Rohne, H.-G. Sander, H. Wachsmuth, C. Zeitnitz

Institut für Physik, Universität Mainz, D-55099 Mainz, Germany[16]

A. Bonissent, J. Carr, P. Coyle, O. Leroy, P. Payre, D. Rousseau, M. Talby

Centre de Physique des Particules, Université de la Méditerranée, IN^2*P*^{3}*-CNRS, F-13288 Marseille, France*

M. Aleppo, F. Ragusa

Dipartimento di Fisica, Università di Milano e INFN Sezione di Milano, I-20133 Milano, Italy

H. Dietl, G. Ganis, A. Heister, K. Hüttmann, G. Lütjens, C. Mannert, W. Männer, H.-G. Moser, S. Schael, R. Settles,[1] H. Stenzel, W. Wiedenmann, G. Wolf

Max-Planck-Institut für Physik, Werner-Heisenberg-Institut, D-80805 München, Germany[16]

P. Azzurri, J. Boucrot,[1] O. Callot, S. Chen, A. Cordier, M. Davier, L. Duflot, J.-F. Grivaz, Ph. Heusse, A. Jacholkowska,[1] F. Le Diberder, J. Lefrançois, A.-M. Lutz, M.-H. Schune, J.-J. Veillet, I. Videau,[1] C. Yuan, D. Zerwas

Laboratoire de l'Accélérateur Linéaire, Université de Paris-Sud, IN^2*P*^{3}*-CNRS, F-91898 Orsay Cedex, France*

G. Bagliesi, T. Boccali, G. Calderini, V. Ciulli, L. Foà, A. Giassi, F. Ligabue, A. Messineo, F. Palla,[1] G. Rizzo, G. Sanguinetti, A. Sciabà, G. Sguazzoni, R. Tenchini,[1] A. Venturi, P.G. Verdini

Dipartimento di Fisica dell'Università, INFN Sezione di Pisa, e Scuola Normale Superiore, I-56010 Pisa, Italy

G.A. Blair, G. Cowan, M.G. Green, T. Medcalf, J.A. Strong, J.H. von Wimmersperg-Toeller

Department of Physics, Royal Holloway & Bedford New College, University of London, Surrey TW20 OEX, United Kingdom[10]

R.W. Clifft, T.R. Edgecock, P.R. Norton, I.R. Tomalin

Particle Physics Dept., Rutherford Appleton Laboratory, Chilton, Didcot, Oxon OX11 OQX, United Kingdom[10]

B. Bloch-Devaux, P. Colas, S. Emery, W. Kozanecki, E. Lançon, M.-C. Lemaire, E. Locci, P. Perez, J. Rander, J.-F. Renardy, A. Roussarie, J.-P. Schuller, J. Schwindling, A. Trabelsi,[21] B. Vallage

CEA, DAPNIA/Service de Physique des Particules, CE-Saclay, F-91191 Gif-sur-Yvette Cedex, France[17]

S.N. Black, J.H. Dann, R.P. Johnson, H.Y. Kim, N. Konstantinidis, A.M. Litke, M.A. McNeil, G. Taylor

Institute for Particle Physics, University of California at Santa Cruz, Santa Cruz, CA 95064, USA[13]

C.N. Booth, S. Cartwright, F. Combley, M. Lehto, L.F. Thompson

Department of Physics, University of Sheffield, Sheffield S3 7RH, United Kingdom[10]

K. Affholderbach, A. Böhrer, S. Brandt, C. Grupen,[1] A. Misiejuk, G. Prange, U. Sieler

Fachbereich Physik, Universität Siegen, D-57068 Siegen, Germany[16]

G. Giannini, B. Gobbo

Dipartimento di Fisica, Università di Trieste e INFN Sezione di Trieste, I-34127 Trieste, Italy

J. Rothberg, S. Wasserbaech

Experimental Elementary Particle Physics, University of Washington, Seattle, WA 98195 U.S.A.

S.R. Armstrong, K. Cranmer, P. Elmer, D.P.S. Ferguson, Y. Gao, S. González, O.J. Hayes, H. Hu,

S. Jin, J. Kile, P.A. McNamara III, J. Nielsen, W. Orejudos, Y.B. Pan, Y. Saadi, I.J. Scott, J. Walsh, Sau Lan Wu, X. Wu, G. Zobernig

Department of Physics, University of Wisconsin, Madison, WI 53706, USA[11]

[1]Also at CERN, 1211 Geneva 23, Switzerland.
[2]Now at Université de Lausanne, 1015 Lausanne, Switzerland.
[3]Also at Dipartimento di Fisica di Catania and INFN Sezione di Catania, 95129 Catania, Italy.
[4]Also Istituto di Fisica Generale, Università di Torino, 10125 Torino, Italy.
[5]Also Istituto di Cosmo-Geofisica del C.N.R., Torino, Italy.
[6]Supported by the Commission of the European Communities, contract ERBFMBICT982894.
[7]Supported by CICYT, Spain.
[8]Supported by the National Science Foundation of China.
[9]Supported by the Danish Natural Science Research Council.
[10]Supported by the UK Particle Physics and Astronomy Research Council.
[11]Supported by the US Department of Energy, grant DE-FG0295-ER40896.
[12]Now at Departement de Physique Corpusculaire, Université de Genève, 1211 Genève 4, Switzerland.
[13]Supported by the US Department of Energy, grant DE-FG03-92ER40689.
[14]Also at Rutherford Appleton Laboratory, Chilton, Didcot, UK.
[15]Permanent address: Universitat de Barcelona, 08208 Barcelona, Spain.
[16]Supported by the Bundesministerium für Bildung, Wissenschaft, Forschung und Technologie, Germany.
[17]Supported by the Direction des Sciences de la Matière, C.E.A.
[18]Supported by the Austrian Ministry for Science and Transport.
[19]Now at SAP AG, 69185 Walldorf, Germany.
[20]Now at Harvard University, Cambridge, MA 02138, U.S.A.
[21]Now at Département de Physique, Faculté des Sciences de Tunis, 1060 Le Belvédère, Tunisia.
[22]Now at Department of Physics, Ohio State University, Columbus, OH 43210-1106, U.S.A.
[23]Also at Dipartimento di Fisica e Tecnologie Relative, Università di Palermo, Palermo, Italy.

1 Introduction

Measurements of the individual b hadron lifetimes represent an important test of the present knowledge of nonspectator effects in the b hadron decay dynamics, such as Pauli interference, W exchange and weak annihilation. Based on the heavy quark expansion formalism, the difference between the lifetimes of the b baryons and mesons is predicted to depend on $1/m_b^2$ and higher order terms, whereas meson-meson differences depend only on $1/m_b^3$ and higher order terms [1]. The predicted hierarchy is $\tau_{\Lambda_b} < \tau_{\bar{B}^0} \sim \tau_{B_s} < \tau_{B^-}$. Differences are expected to be at the level of a few percent, which sets the scale of the experimental precision required.

This paper reports an improved measurement of the $\bar{B}^0$ and B^- lifetimes with the ALEPH detector at LEP, using approximately four million hadronic decays of the Z, collected in the period 1991–1995. This data sample was recently reprocessed, achieving higher efficiency and better resolution in the track reconstruction, which is highly beneficial for this analysis.

Semileptonic decays of $\bar{B}^0$ and B^- mesons are partially reconstructed by identifying events containing a lepton (electron or muon) with an associated D^0 or $D^{\star+}$ meson. The resulting D^0-lepton ($D^0\ell^-$) and $D^{\star+}$-lepton ($D^{\star+}\ell^-$) event samples consist mostly of B^- and $\bar{B}^0$ decays, respectively (charge conjugate modes are implied throughout this paper).

Previous measurements of the $\bar{B}^0$ and B^- lifetimes are reported in [2, 3].

2 The ALEPH detector

A detailed description of the ALEPH detector can be found elsewhere [4, 5]. A high resolution vertex detector (VDET) consisting of two layers of silicon with double-sided readout provides measurements in the $r\phi$ and z directions at average radii of 6.5 cm and 11.3 cm, with 12 μm precision at normal incidence. The VDET provides full azimuthal coverage, and polar angle coverage to $|\cos\theta| < 0.85$ for the inner layer only and $|\cos\theta| < 0.69$ for both layers. Outside the VDET, particles traverse the inner tracking chamber (ITC) and the time projection chamber (TPC). The ITC is a cylindrical drift chamber with eight axial wire layers at radii of 16 to 26 cm. The TPC measures up to 21 space points per track at radii between 40 and 171 cm, and also provides a measurement of the specific ionization energy loss (dE/dx) of each charged track. These three detectors form the tracking system, which is immersed in a 1.5 T axial magnetic field provided by a superconducting solenoid. The combined tracking system yields a momentum resolution transverse to the beam axis of $\sigma(p_T)/p_T = 6 \times 10^{-4}\ p_T \oplus 0.005$ (p_T in GeV/c). The resolution of the three-dimensional impact parameter for tracks having two VDET hits can be parametrized as $\sigma = 25\ \mu\text{m} + 95\ \mu\text{m}/p$ (p in GeV/c) [6].

The electromagnetic calorimeter (ECAL) is a lead/wire-chamber sandwich operated in proportional mode. The calorimeter is read out in projective towers that subtend typically $0.9^\circ \times 0.9^\circ$ in solid angle, segmented in three longitudinal sections. The hadron calorimeter (HCAL) uses the iron return yoke as absorber. Hadronic showers are sampled by 23 planes of streamer tubes, with analogue projective tower and digital hit pattern readout. The HCAL is used in combination with two double layers of muon chambers outside the magnet for muon identification.

Recently the LEP1 data were reprocessed using improved reconstruction algorithms. The features that are particularly relevant for the enhancement of the charmed meson reconstruction efficiency are the following. A new VDET pattern recognition algorithm allows groups of several nearby tracks which may share common hits to be analysed together, to find the hit assignments that minimize the overall χ^2 for the event. The improvement in the hit association efficiency is more than 2% (from 89.2% to 91.0% in $r\phi$ and from 85.6% to 88.2% in z). Information on the drift time from the TPC wires is combined with that obtained from the pads to reduce the error in the z coordinate by a factor of two. A 30% improvement in the $r\phi$ coordinate resolution is achieved for low momentum tracks by correcting the pad coordinates for ionisation fluctuations along the tracks as measured by the wires. The particle identification (dE/dx) is improved by combining pulse height data from the TPC pads with that of the wires. The improvements in the charmed meson reconstruction efficiencies with respect to the previous analysis range from 10 to 30%, depending on the decay channel.

3 Event selection

The $D^{\star+}\ell^-$ and $D^0\ell^-$ event samples consist of an identified lepton (e or μ) associated with a fully reconstructed $D^{\star+}$ or D^0 candidate. The selection of muons and electrons is described in detail in [7]. For this analysis, lepton candidates are required to have a momentum of at least 2.0 GeV/c for electrons and 2.5 GeV/c for muons.

The $D^{\star+}$ and D^0 candidates are reconstructed from charged tracks and π^0's that form an angle of less than 45° with the lepton candidate. These charged tracks are also required to intersect a cylinder of radius 2 cm and half-length 4 cm centered on the nominal interaction point, to have at least 4 hits in the TPC, a polar angle θ such that $|\cos\theta| < 0.95$ and a transverse momentum greater than 200 MeV/c.

Photons and π^0's are identified in the ECAL. The four-momenta of π^0 candidates are computed by adding the photon momenta when the $\gamma\gamma$ invariant mass is consistent with the π^0 mass. The energy of the π^0 is then recomputed using the kinematical constraint of the π^0 mass [6]. The energy resolution achieved is about 6.5%, almost independent of the energy. For reconstructing the D^0 candidates, only π^0's with momenta greater than 2 GeV/c are used.

For all charged kaons used to reconstruct the D^0 it is required that the dE/dx be within 3σ of that expected from a kaon, except for the $D^{\star+} \to D^0\pi^+$, $D^0 \to K^-\pi^+$decay channel. The kaon has the same sign as the lepton coming from the B semileptonic decay, therefore this charge correlation is required.

$K^0_{\rm S}$ candidates are reconstructed from pairs of oppositely charged tracks. The two tracks are required to be inconsistent with originating from the interaction point and the $K^0_{\rm S}$ candidate is rejected if the measured mass is more than 2σ (± 10 MeV/c^2) from the nominal $K^0_{\rm S}$ mass.

Tracks coming from the D^0 decays are required to form a common vertex with a χ^2 confidence level greater than 1%. In the D^0 decay channels that do not contain a π^0 in the final state, if more than one combination satisfies the selection criteria, the one with the smallest χ^2 of the D vertex fit is selected. For the decay modes where the

multiple candidates originate from different π^0 combinations, for a given detected lepton, the candidate with $m_{D^0\pi} - m_{D^0}$ closest to the nominal value is chosen in case of $D^\star$ selection, otherwise the highest momentum D^0 candidate is chosen.

In order to reject the background from charm, to improve the signal to background ratio and to ensure well-measured decay lengths, additional selection criteria are applied to all the subsamples. The invariant mass of the $D^{(\star)}\ell$ system is required to be greater than 3 GeV/c^2, where $D^{(\star)}$ can be $D^{\star+}$ or D^0. This cut significantly reduces the charm background while keeping $\sim 85\%$ of the signal. To exploit the high precision of the silicon vertex detector, the lepton track and at least two tracks from the D^0 decay are required to have at least one VDET hit in both the $r\phi$ and z projections.

3.1 The $D^\star$-lepton selection

$D^{\star+}$ candidates are identified via the decay $D^{\star+} \to D^0\pi^+$, followed by $D^0 \to K^-\pi^+$, $D^0 \to K^-\pi^+\pi^-\pi^+$, $D^0 \to K^-\pi^+\pi^0$ or $D^0 \to K^0_S\pi^+\pi^-$. The difference in mass between the $D^{\star+}$ and D^0 candidates must lie within 1.5 MeV/c^2 (approximately two standard deviations of the experimental resolution) of the nominal value of 145.4 MeV/c^2.

In the $D^0 \to K^-\pi^+$ channel, the D^0 momentum p_{D^0} is required to be greater than 5 GeV/c.

For the $D^0 \to K^-\pi^+\pi^-\pi^+$ channel p_{D^0} must be greater than 8 GeV/c, and at least two of the D^0 decay tracks must have $p > 1$ GeV/c.

In the case of the $D^0 \to K^-\pi^+\pi^0$ channel, the momentum of the reconstructed D^0 is required to be greater than 10 GeV/c, and the two charged tracks in the decay are required to have $p > 0.5$ GeV/c. Futhermore the decay kinematics are required to be consistent with one of the three resonant decays: $D^0 \to K^-\rho^+$, $D^0 \to K^{\star-}\pi^+$, $D^0 \to \bar{K}^{\star0}\pi^0$. For each decay hypothesis the mass of the resonant particle and the helicity angle θ_H are calculated[1]. If the mass is consistent with the nominal resonance mass value, within its natural width, and if $|\cos\theta_H| > 0.4$, the candidate is considered to be consistent with the resonant decay hypothesis. For these resonant decays a $\cos^2\theta_H$ distribution is expected.

Finally, in the $D^0 \to K^0_S\pi^+\pi^-$ channel, the momentum of the reconstructed D^0 is required to be greater than 4 GeV/c. The same technique as in the $D^0 \to K^-\pi^+\pi^0$ channel is used to tag the $K^{\star-}$ resonance. The sign of the resonance is used to distinguish between D^0 and $\bar{D}^0$.

3.2 The D^0-lepton selection

The $D^0\ell^-$ sample consists of events with a lepton and a D^0 candidate, where the D^0 is not the decay product of a reconstructed $D^{\star+}$. The D^0 candidates are identified using the same decay modes as for the $D^{\star+}\ell^-$sample. For this sample, the background is larger because the $D^{\star+}$–D^0 mass difference criterion is not applicable.

For all the decay modes selected in the $D^0\ell^-$sample, a search for the additional pion is performed to reject D^0 candidates coming from $D^{\star+} \to D^0\pi^+$. If a pion candidate is

[1]The helicity angle θ_H is defined as the angle between the scalar particle and one of the decay products of the vector particle, calculated in the rest frame of the vector particle.

found yielding a $D^{\star+}$–D^0 mass difference within 6 MeV/c^2 of the nominal value, the $D^0\ell^-$ candidate is rejected. The efficiency for reconstructing the additional pion and rejecting D^0's coming from $D^{\star+}$ decays is found to be 86% from the Monte Carlo simulation.

In the $D^0 \to K^-\pi^+$ channel, the reconstructed D^0's are required to have $\mathrm{p}_{D^0} > 8$ GeV/c, $p_K > 2$ GeV/c and $p_\pi > 1.5$ GeV/c. In the $D^0 \to K^-\pi^+\pi^-\pi^+$ channel the D^0 momentum is required to exceed 12 GeV/c while the kaon and the three pions must have momenta greater than 2 and 1 GeV/c, respectively.

The cuts on the kaon and pion momenta are tightened for the $D^0 \to K^-\pi^+\pi^0$ channel, to $p_K > 3$ GeV/c and $p_\pi > 2$ GeV/c, while the reconstructed D^0 must have $\mathrm{p}_{D^0} > 12$ GeV/c. The same cuts on the three resonances are used as in the $D^{\star+}\ell^-$event sample.

Finally, for the $D^0 \to K^0_S\pi^+\pi^-$ channel a cut is applied of at least 1.5 GeV/c on the kaon momentum and 1.0 GeV/c on the two pion momenta. The momentum of the reconstructed D^0 candidates is required to be greater than 10 GeV/c. The same technique is used to tag the $K^{\star-}$ resonance as in the $D^{\star+}\ell^-$ event sample.

3.3 *B* meson reconstruction

The B decay vertex position is estimated by vertexing the reconstructed D^0 track with the lepton. Events are rejected if the B vertex fit gives a χ^2 probability less than 1%.

The D^0 candidate mass spectra for the four subsamples in the $D^{\star+}\ell^-$ event selection are shown in Fig. 1, and in the $D^0\ell^-$ event selection in Fig. 2. The fitted curves consist of a Gaussian function for the signal plus a linear background. For the $D^0 \to K^-\pi^+\pi^0$ in the $D^0\ell^-$sample a Gaussian tail is used to describe the background; masses below 1.65 GeV/c^2 are excluded to avoid the broad enhancement due to the missing π^0 in the $D^0 \to K^-\pi^+\pi^0\pi^0$ decay. The fitted D^0 width and the fitted number of signal and background events within a window of $\pm 2\sigma$ around the fitted mass are shown in Table 1 for the different samples.

Events reconstructed within two standard deviations of the fitted D^0 mass are selected for the lifetime analysis, resulting in 1880 $D^{\star+}\ell^-$ and 2856 $D^0\ell^-$ candidates. The decay length is calculated for these events by reconstructing the primary and B decay vertices in three dimensions. The primary vertex reconstruction algorithm [8] applied to simulated $b\bar{b}$ events yields an average resolution of 50 μm $\times$ 10 μm $\times$ 60 μm (horizontal $\times$ vertical $\times$ beam direction).

The distance between the primary and B decay vertices is projected onto the direction defined by the momentum of the $D^{(\star)}\ell$ system. The uncertainty on the flight direction due to the missing neutrino induces a negligible error on the decay length. The resolution on the B decay length is on average 250 μm, compared with an average B decay length of about 2.5 mm.

For the $D^0 \to K^-\pi^+\pi^0$ channel, the π^0 momentum is included when extrapolating the neutral D^0 track backwards to form the B vertex. In the case of $D^{\star+}\ell^-$ events, the soft pion from the $D^{\star+}$ decay does not improve the resolution on the B decay length and is therefore not used in the reconstruction of the B vertex.

Because the selected decays contain an undetected neutrino, the B momentum is not

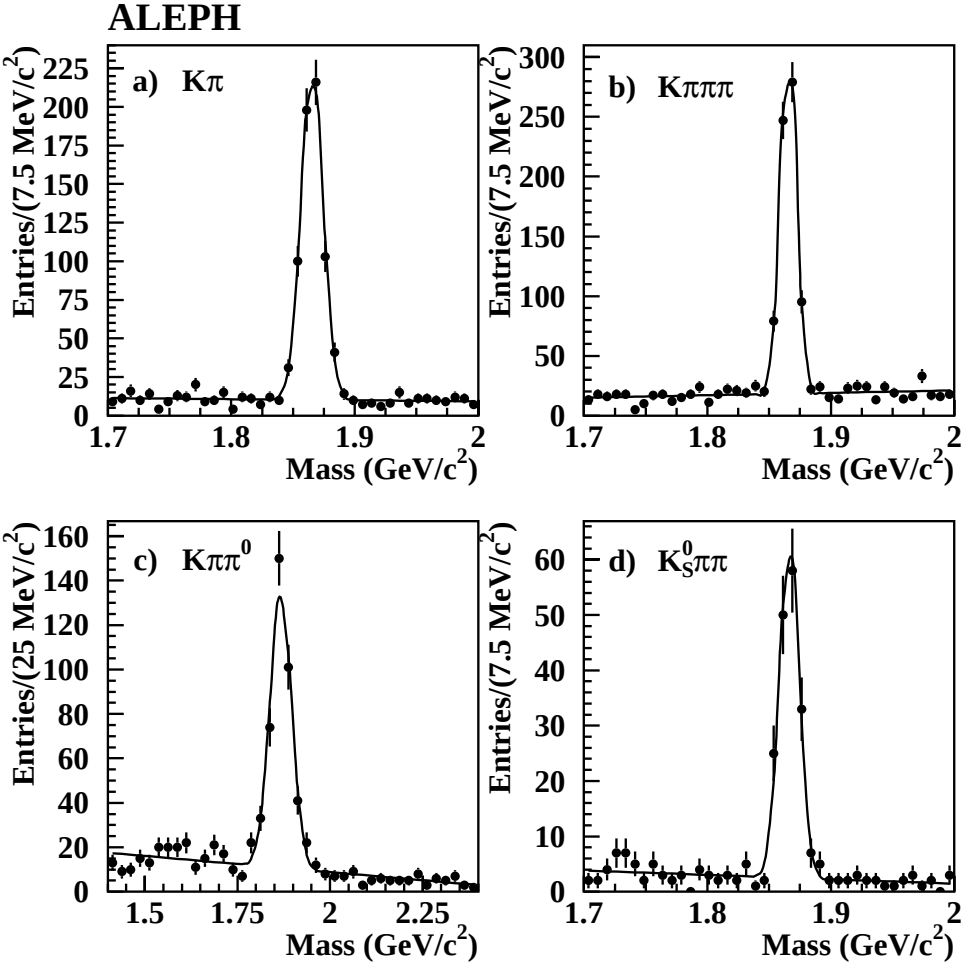

Figure 1: The invariant mass of D^0 candidates for the four subsamples in the $D^{\star+}\ell^-$ event selection: a) $D^0 \to K^-\pi^+$, b) $D^0 \to K^-\pi^+\pi^-\pi^+$, c) $D^0 \to K^-\pi^+\pi^0$ (notice the different mass scale), d) $D^0 \to K^0_S\pi^-\pi^+$. The superimposed curves are the results of the fit described in the text.

known precisely and is reconstructed using an energy flow technique as described in [9]. A further correction is applied by evaluating for Monte Carlo events the κ distribution, defined as

$$\kappa = \frac{(\beta\gamma)_{\rm reco}}{(\beta\gamma)_B}. \tag{1}$$

Because this distribution depends on the selection criteria applied, separate κ distributions are calculated for each subsample. The momentum resolution obtained is between 8 and 10%, depending on the decay channel.

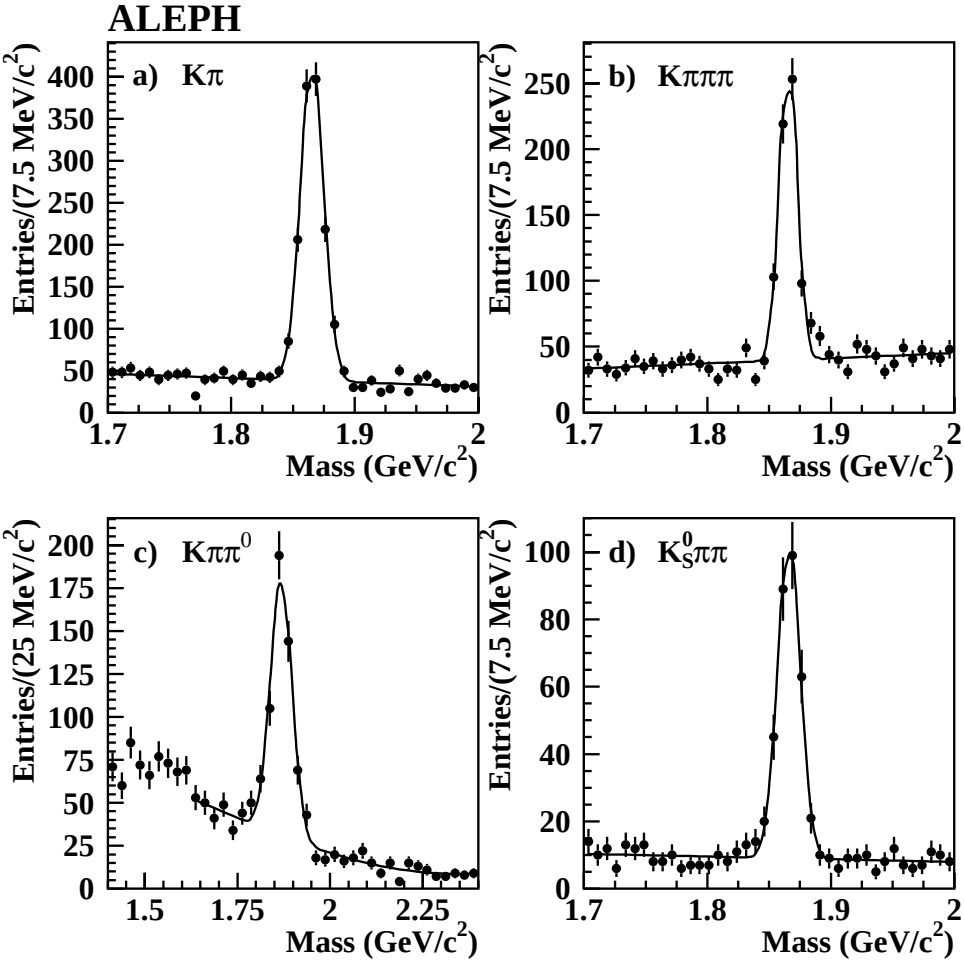

Figure 2: The invariant mass of D^0 candidates for the four subsamples in the $D^0\ell^-$ event selection: a) $D^0 \to K^-\pi^+$, b) $D^0 \to K^-\pi^+\pi^-\pi^+$, c) $D^0 \to K^-\pi^+\pi^0$ (notice the different mass scale), d) $D^0 \to K^0_S\pi^+\pi^-$. The superimposed curves are the results of the fit described in the text.

4 Lifetime measurement

An unbinned likelihood fit for the lifetimes is performed. For each event the probability of observing a proper time t given the lifetime τ is calculated: the probability density function $F(t, \sigma_t, \tau)$ is obtained by convoluting an exponential distribution with the properly normalised κ distribution and with a Gaussian function which takes into account the resolution on the decay length.

Both the $D^{\star+}\ell^-$ and $D^0\ell^-$ samples contain a mixture of $\bar{B}^0$ and B^- decays and the $B^-/\bar{B}^0$ mixture in the samples depends on the ratio of the lifetimes, as discussed in Section 4.2. Therefore, to measure the $\bar{B}^0$ and B^- lifetimes a simultaneous maximum likelihood fit is performed to all the events. The likelihood function contains three components for

Table 1: Fitted D^0 width (σ), number of D^0 candidates and fraction of background events falling within a mass window of $\pm 2\sigma$. The uncertainties are statistical only.

Subsample		Width (MeV/c^2)	Candidate events	Background fraction
$D^{\star+}\ell^-$	$D^0 \to K^-\pi^+$	8.6 ± 0.3	651	0.066 ± 0.004
	$D^0 \to K^-\pi^+\pi^-\pi^+$	6.6 ± 0.3	670	0.096 ± 0.004
	$D^0 \to K^-\pi^+\pi^0$	30.3 ± 1.6	394	0.127 ± 0.008
	$D^0 \to K^0_S\pi^+\pi^-$	8.3 ± 0.7	165	0.061 ± 0.006
$D^0\ell^-$	$D^0 \to K^-\pi^+$	8.7 ± 0.3	1312	0.133 ± 0.006
	$D^0 \to K^-\pi^+\pi^-\pi^+$	7.2 ± 0.5	664	0.232 ± 0.012
	$D^0 \to K^-\pi^+\pi^0$	28.4 ± 1.9	563	0.258 ± 0.012
	$D^0 \to K^0_S\pi^+\pi^-$	8.6 ± 0.8	317	0.139 ± 0.009

each sample and is written as

$$\begin{aligned}\mathcal{L} &= \prod_{i=1}^{N_{D^{\star}\ell}} \left[f^{\star}_{-}(\tau_{B^-}/\tau_{\bar{B}^0}) F(t_i, \sigma_i, \tau_{B^-}) + f^{\star}_{0}(\tau_{B^-}/\tau_{\bar{B}^0}) F(t_i, \sigma_i, \tau_{\bar{B}^0}) + f^{\star}_{\rm bkg} F^{\star}_{\rm bkg}(t_i) \right] \\ &\times \prod_{i=1}^{N_{D^0\ell}} \left[f^{0}_{-}(\tau_{B^-}/\tau_{\bar{B}^0}) F(t_i, \sigma_i, \tau_{B^-}) + f^{0}_{0}(\tau_{B^-}/\tau_{\bar{B}^0}) F(t_i, \sigma_i, \tau_{\bar{B}^0}) + f^{0}_{\rm bkg} F^{0}_{\rm bkg}(t_i) \right] . \quad (2)\end{aligned}$$

The coefficients $f^{\star}_{-}$ and $f^{\star}_{0}$ are the fractions of the $D^{\star+}\ell^-$ sample arising from B^- and $\bar{B}^0$ decays, respectively. Similarly, f^{0}_{-} and f^{0}_{0} are the fractions of B^- and $\bar{B}^0$ decays in the $D^0\ell^-$ sample. The coefficients $f^{\star}_{\rm bkg}$ and $f^{0}_{\rm bkg}$ are the background fractions of the samples, while the functions $F^{\star}_{\rm bkg}(t)$ and $F^{0}_{\rm bkg}(t)$ are their normalised proper time distributions.

4.1 Backgrounds

Background contamination arises from the following sources:

(1) combinatorial background, i.e. candidates with a fake $D^{(\star)}$;

(2) the process $\bar{B} \to D^-_s D^{(*)} X$, followed by $D^-_s \to \ell^- X$, giving rise to a real $D^{(\star)}$ and a real lepton;

(3) a real $D^{(\star)}$ meson accompanied by a fake or nonprompt lepton, from $Z \to b\bar{b}$ or $Z \to c\bar{c}$ events.

Source (1) is the dominant background. Its contribution is determined from a fit to the D^0 mass distributions, and its magnitude is given in Table 1 for the various subsamples. The proper time distribution for this source is determined from the data by selecting events from the high mass sideband of the D^0 peak. The same selection criteria described

in Section 3 are applied to the background samples, except that the requirement on the $D^{\star+}$–D^0 mass difference in the case of the $D^{\star+}\ell^-$ events is removed to increase the statistics. A function consisting of a Gaussian plus positive and negative exponential tails is used to describe these data.

The contribution from source (2) is calculated from the measured branching ratios for this process [10] and a Monte Carlo simulation to determine the detection efficiency; it accounts for a contamination which is about 2–3% of the sample, depending on the channel.

The background from source (3) is estimated from the measured hadron-lepton misidentification probabilities [7] and the measured inclusive D^0 and $D^{\star+}$ rates. An independent estimate is obtained using wrong-sign ($D^{\star+}\ell^+$ or $D^0\ell^+$) events, and is found to be consistent. This background source contributes between 2 and 5% of the sample, depending on the channel. To characterize the proper time distribution of this background, it is further subdivided into three distinct components: fake leptons coming from the primary vertex in $c\bar{c}$ and $b\bar{b}$ events, and fake leptons coming from a decaying b hadron.

The proper time distribution for sources (2) and (3) are determined from simulated events.

4.2 Sample compositions

Both the $D^{\star+}\ell^-$ and $D^0\ell^-$ samples contain a mixture of $\bar{B}^0$ and B^- decays. In order to estimate the cross contamination, the individual semileptonic branching ratios of the $\bar{B}^0$ and B^- must be determined. The evaluation follows the same procedure as given in the appendix of [2]. An important input in this evaluation is the knowledge of the branching ratios for the decay modes $B \to D^{\star\star}\pi\ell\nu$, where $D^{\star\star}$ represents any of the p−wave resonances as well as the nonresonant $D^{(\star)}\pi$ states. The most recent ALEPH and DELPHI results [11, 12] for both the resonant and the nonresonant components are used in the calculation, leading to a significant reduction in the resulting uncertainty compared to the previous analysis of [2]. The $\bar{B}^0$ and B^- content of the two samples are calculated using as input the measured values of the branching ratios given in Table 2. The sample composition is then calculated by considering the $\bar{B}^0$ and B^- decay channels that contribute to the $D^{\star+}\ell^-$ and $D^0\ell^-$ samples [2, 14], taking into account the probability of 0.147 ± 0.015 that a $D^{\star+}\ell^-$ event is mistakenly reconstructed as a $D^0\ell^-$ event.

As a consequence of this procedure, the coefficients $f_-^\star$, $f_0^\star$, f_-^0 and f_0^0 appearing in the likelihood function (Eq. 2) depend on the lifetime ratio. For equal lifetimes, about 85% of the B decays in the $D^{\star+}\ell^-$ sample are attributed to $\bar{B}^0$, while about 80% of the $D^0\ell^-$ sample B decays come from B^-.

4.3 Fit results

The fit to the proper time distributions of the $D^{\star+}\ell^-$ and $D^0\ell^-$ events is performed to determine the two free parameters $\tau_{\bar{B}^0}$ and τ_{B^-}. The values obtained are

$$\tau_{\bar{B}^0} \;=\; 1.518 \pm 0.053 \text{ ps},$$

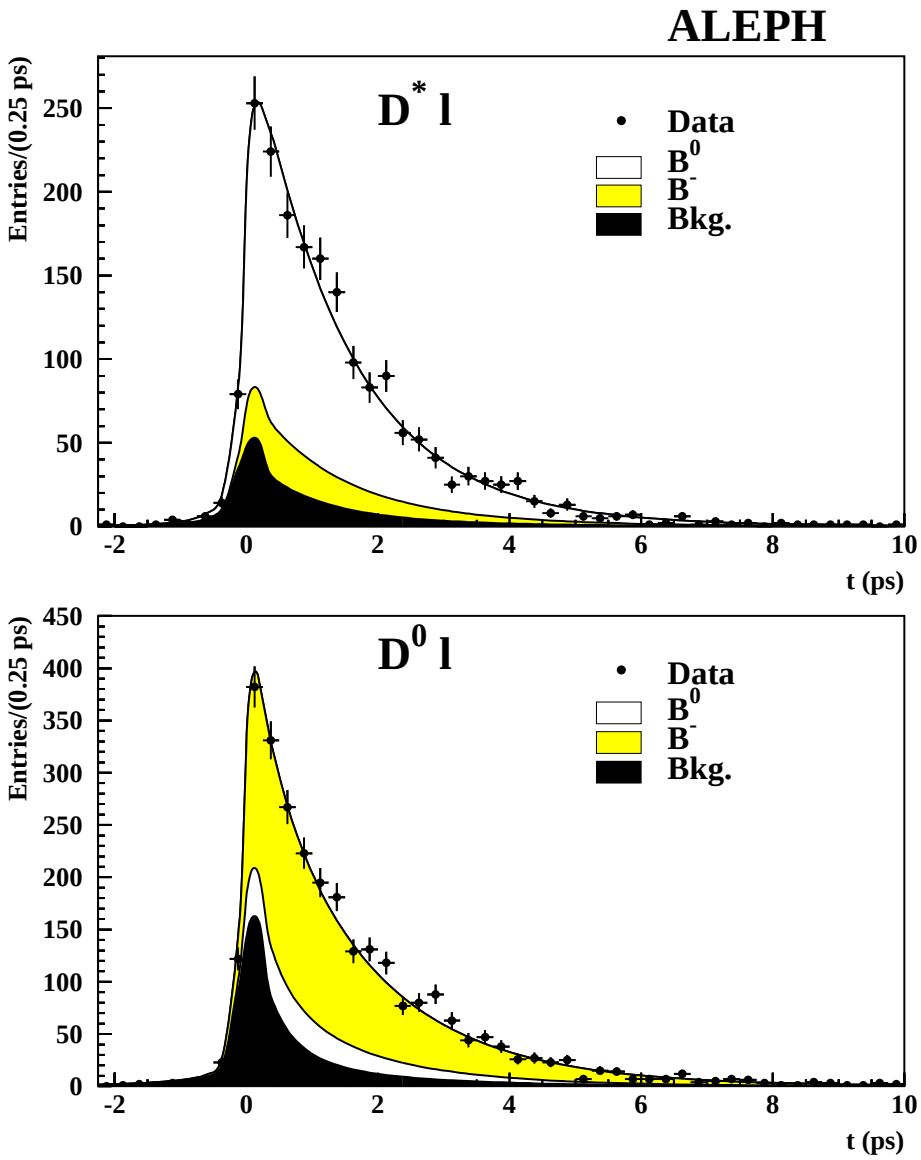

Figure 3: Proper time distributions with the result of the fit overlaid for the two samples. The plots show the background contributions to the samples, together with the $\bar{B}^0$ and B^- components.

$$\tau_{B^-} \quad = \quad 1.648 \pm 0.049 \text{ ps},$$

where the errors are statistical only. The statistical correlation coefficient is -0.35. The ratio of the lifetimes is

$$\tau_{B^-}/\tau_{\bar{B}^0} = 1.085 \pm 0.059,$$

taking into account the correlation.

The proper time distributions for the two samples are shown in Fig. 3, with the results of the fit overlaid.

4.4 Systematic uncertainties

The sources of systematic uncertainty are discussed in the following, and the estimated errors are summarized in Table 3.

The uncertainty in the B momentum reconstruction is dominated by the uncertainty in the κ distribution. The effects that can modify the κ function with a consequence on the extracted lifetimes are studied. The first is due to the $D^{(\star)}\pi$ content of semileptonic B decays, which affects the κ function due to the smaller phase space available and the softer momentum spectrum of the reconstructed $D^{(\star)}\ell$ system. The fractions of $D^{(\star)}\pi$ decays are varied in the simulation within experimental errors. Other effects studied are the dependence of the κ distribution on the analysis cuts and the b fragmentation function. These two effects combined give a relative uncertainty of about 2% in the B momentum determination. Uncertainties in the κ distribution propagate in the same way to τ_{B^-} and $\tau_{\bar{B}^0}$, and therefore have a small effect in the ratio.

Uncertainties in the background fractions and proper time distributions are considered. The combinatorial background, estimated in the data from fits to the D^0 mass spectra, is reported in Table 1 for each individual channel. The systematic uncertainty due to this source is estimated by varying the combinatorial background in the fit for each channel within its statistical errors in turn and taking the sum in quadrature. The contamination from physics background is evaluated using the simulation, by varying the fraction within the estimated uncertainty and repeating the fits. The uncertainty on the total background level is calculated by combining the two above sources.

The parameters describing the background proper time distributions are varied within their uncertainties. Background proper time distributions are parametrized using different methods, to check for possible systematic bias. Different background samples are selected by varying the sideband regions, adding events from the lower sideband, which are excluded in the lifetime determination, or using events with wrong-sign correlations. Some cuts in the selection are varied to check the stability of the parametrizations. The shapes extracted from real data are compared with those extracted from Monte Carlo events. The resulting differences in the fitted lifetimes are used to estimate the systematic uncertainty.

For the remaining systematic errors, which are small compared to the statistical ones, the correlation between the lifetimes is not propagated into the ratio.

The systematic uncertainty due to the sample compositions is determined by varying the branching fractions of Table 2 within $\pm 1\sigma$ from the central values. In addition the uncertainty due to the assumption of isospin conservation has been estimated, allowing for a variation of 20% relative to the exact symmetry.

As explained in detail in [2], a small fraction of four-body decays where an extra pion is produced in the decay of the B meson contributes to the sample composition, and is characterized by a different selection efficiency with respect to the real signal. The relative efficiencies

$$\frac{\epsilon(B \to D^{(\star)}\pi\ell\nu)}{\epsilon(B \to D^{(\star)}\ell\nu)} = 0.75 \pm 0.10 \text{ (for } \bar{B}^0) \qquad 0.64 \pm 0.10 \text{ (for } B^-)$$

therefore enter into the calculation and this uncertainty (coming from the limited Monte Carlo statistics) is propagated to the measured lifetimes.

Table 2: Branching ratios used as input values in the calculation of the sample composition.

Decay	B.R.	Reference
$\bar{B}^0 \to D^{\star+}\ell^-\bar{\nu}$	0.0460 ± 0.0027	[13]
$\bar{B}^0 \to D^{+}\ell^-\bar{\nu}$	0.0200 ± 0.0025	[13]
$\bar{B}^0 \to \ell^-\bar{\nu}X$	0.1045 ± 0.0021	[13]
$\bar{B}^0 \to D^0\pi^+\ell^-\bar{\nu}$ + $\bar{B}^0 \to D^{\star 0}\pi^+\ell^-\bar{\nu}$	0.0159 ± 0.0036	[11, 12]
$B^- \to D^{\star+}\pi^-\ell^-\bar{\nu}$	0.0121 ± 0.0018	[11, 12]
$B^- \to D^{+}\pi^-\ell^-\bar{\nu}$	0.0124 ± 0.0048	[12]
$B^- \to D^{+}\pi^-\ell^-\bar{\nu}$ + $B^- \to D^{\star+}\pi^-\ell^-\bar{\nu}$	0.0157 ± 0.0031	[11]

Table 3: Sources of systematic error on the fitted lifetimes.

Source of error	Contribution to systematic error		
	$\tau_{\bar{B}^0}$ (ps)	τ_{B^-} (ps)	$\tau_{B^-}/\tau_{\bar{B}^0}$
B momentum reconstruction	± 0.025	± 0.026	± 0.009
Background treatment	± 0.020	± 0.020	± 0.010
Sample compositions	± 0.003	± 0.003	± 0.004
$D^{(\star)}\pi\ell^-\nu$ relative efficiency	± 0.006	± 0.006	± 0.006
Decay length resolution	± 0.008	± 0.008	± 0.008
Total	± 0.034	± 0.035	± 0.018

The parameters of the decay length resolution function are varied within their errors to estimate the resulting uncertainty [14].

5 Conclusions

The lifetimes of the charged and neutral B mesons have been measured with the full statistics collected by the ALEPH detector at and around the Z peak energy. The data sample was recently reprocessed, achieving improved tracking performance. A maximum likelihood fit to the proper time distributions of 1880 $D^{\star+}\ell^-$ and 2856 $D^0\ell^-$ candidates yields the following results for the $\bar{B}^0$ and B^- lifetimes and their ratio:

$$\begin{aligned} \tau_{\bar{B}^0} &= 1.518 \pm 0.053 \pm 0.034 \text{ ps}, \\ \tau_{B^-} &= 1.648 \pm 0.049 \pm 0.035 \text{ ps}, \end{aligned}$$

$$\tau_{B^-}/\tau_{\bar{B}^0} = 1.085 \pm 0.059 \pm 0.018 \ ,$$

where the first error is statistical and the second is systematic.

These results supersede the corresponding ones of [2]. Averaging with the results of the other methods presented in [2] the combined values are:

$$\begin{aligned} \tau_{\bar{B}^0} &= 1.496 \pm 0.048 \pm 0.033 \text{ ps}, \\ \tau_{B^-} &= 1.644 \pm 0.048 \pm 0.034 \text{ ps}, \\ \tau_{B^-}/\tau_{\bar{B}^0} &= 1.104 \pm 0.057 \pm 0.019. \end{aligned}$$

Acknowledgments

We thank our colleagues in the accelerator divisions for the excellent performance of LEP. Thanks also to the many engineering and technical personnel at CERN and at the home institutes for their contributions to the performance of the ALEPH detector. Those of us from non-member states thank CERN for its hospitality.

References

[1] I. Bigi, N. Uraltsev, *Gluonic enhancements in non-spectator beauty decays: an inclusive mirage though an exclusive possibility*, Phys. Lett. **B280** (1992) 271;
I. Bigi, M. Shifman and N. Uraltsev, *Aspects of heavy quark theory*, Ann. Rev. Nucl. Part. Sci. **47** (1997) 591, and references therein;
M. Neubert and C.T. Sachrajda, *Spectator effects in inclusive decays of beauty hadrons*, Nucl. Phys. **B483** (1997) 339.

[2] ALEPH Collaboration, *Improved measurement of the $\bar{B}^0$ and B^- meson lifetimes*, Z. Phys. **C71** (1996) 31.

[3] CDF Collaboration, *Measurement of the B^- and $\bar{B}^0$ meson lifetimes using semileptonic decays*, Phys. Rev. **D58** (1998) 092002;
CDF Collaboration, *Measurement of B hadron lifetimes using J/ψ final states at CDF*, Phys. Rev. **D57** (1998) 5382;
DELPHI Collaboration, *A measurement of B^+ and B^0 lifetimes using $\bar{D}\ell^+$ events*, Z. Phys. **C68** (1995) 13;
DELPHI Collaboration, *Lifetimes of charged and neutral B hadrons using event topology*, Z. Phys. **C68** (1995) 363.
DELPHI Collaboration, *A precise measurement of the B^0_d meson lifetime using a new technique*, Z. Phys. **C74** (1997) 19;
L3 Collaboration, L3 Note 2142, June 30, 1998. *Measurement of the B^0_d meson lifetime using the decay $\bar{B}^0_d \to D^{\star +} X l \nu$*, paper contributed to the XXIX Int. Conf. on High Energy Physics, July 13–29 1998, Vancouver, Canada;
OPAL Collaboration, *Improved measurement of the B^0 and B^+ meson lifetimes*, Z. Phys. **C67** (1995) 379;
OPAL Collaboration, *Measurement of the B^+ and B^0 lifetimes and search for CP(T)*

violation using reconstructed secondary vertices, CERN–EP/98–195. To be published in Eur. Phys. J. C;
SLD Collaboration, *Measurement of the B^+ and B^0 lifetimes using topological reconstruction of inclusive and semileptonic decays*, Phys. Rev. Lett. **79** (1997) 590.
SLD Collaboration *Measurement of the B^+ and B^0 Lifetimes using Topological Vertexing at SLD*, SLAC-PUB-8206 (July 1999), paper contributed to the International Europhysics Conference on High Energy Physics, July 15–21 1999, Tampere, Finland.

[4] ALEPH Collaboration, *ALEPH: a detector for electron-positron annihilations at LEP*, Nucl. Instr. Meth. **A 294** (1990) 121.

[5] B. Mours *et al.*, *The design, construction and performance of the ALEPH silicon vertex detector*, Nucl. Instr. Meth. **A 379** (1996) 101.

[6] ALEPH Collaboration, *Performance of the ALEPH detector at LEP*, Nucl. Instr. Meth. **A 360** (1995) 481.

[7] ALEPH Collaboration, *Heavy quark tagging with leptons in the ALEPH detector,* Nucl. Instr. Meth. **A 346** (1994) 461.

[8] ALEPH Collaboration, *A precise measurement of $\Gamma(Z \to b\bar{b})/\Gamma(Z \to hadrons)$*, Phys. Lett. **B313** (1993) 535.

[9] ALEPH Collaboration, *Measurement of the effective b quark fragmentation function at the Z resonance*, Phys. Lett. **B357** (1995) 699.

[10] CLEO Collaboration, *Exclusive and inclusive decays of b mesons into D_s mesons,* Phys. Rev. Lett. **64** (1990) 2117.
ARGUS Collaboration, *Production of D_s^+ mesons in b decays and determination of $f(D_s)$,* Z. Phys. **C54** (1992) 1.

[11] ALEPH Collaboration, *Production of orbitally excited charm mesons in semileptonic b decays,* Z. Phys. **C73** (1997) 601.

[12] DELPHI Collaboration, *Measurement of the $\bar{B} \to D^{(\star)}\pi\ell\nu_\ell$ Branching Fraction,* CERN-EP/99-174.

[13] C. Caso *et al.*, Particle Data Group, Eur. Phys. J. **C3** (1998) 1.

[14] G. Calderini, *Measurement of the B^+ and B^0 Meson Lifetimes at ALEPH*, Ph.D. Thesis, Scuola Normale Superiore di Pisa, January 2000.